Int. J. Heat Mass Transfer. Vol. 27, No. 8, pp. 1171–1182, 1984
Printed in Great Britain

0017-9310/84 $3.00 + 0.00

ENDOTHERMIC GASIFICATION OF A SOLID BY THERMAL RADIATION ABSORBED IN DEPTH

W. BÖRSCH-SUPAN
Fachbereich 17 Mathematik, Johannes Gutenberg-Universität, D-6500 Mainz, Federal Republic of Germany

and

L. W. HUNTER† and J. R. KUTTLER
Milton S. Eisenhower Research Center, Applied Physics Laboratory, The Johns Hopkins University, Johns Hopkins Road, Laurel, MD 20707, U.S.A.

(*Received* 24 *June* 1982 *and in revised form* 18 *October* 1983)

Abstract—A model solid is exposed to thermal radiation that penetrates the surface. The solid gasifies in depth by an endothermic reaction with an Arrhenius rate coefficient. The absorption of radiation and the thermal conductivity both depend on the local density. The materials considered are polymeric solids, composites, graphite and metals. The model predicts a monotonic temperature rise through the reaction zone and a surface temperature that depends on the absorption coefficient. This contrasts with earlier predictions of radiant heating especially by high-power lasers.

NOMENCLATURE

A frequency factor in equation (8) [s^{-1}]
$\hat{C}_s$ specific heat of solid [$J\,kg^{-1}\,K^{-1}$]
$\hat{E}$ chemical activation energy per unit mass in equation (8) [$J\,kg^{-1}$]
E^* equation (15)
H total enthalpy per unit volume [$J\,m^{-3}$]
$\hat{H}_s$, $\hat{H}_g$, $\hat{H}$ specific enthalpy of the solid, gas and both, respectively [$J\,kg^{-1}$]
$\Delta\hat{H}$ specific heat of reaction, equation (3) [$J\,kg^{-1}$]
I_∞ absorbed intensity of thermal radiation [$J\,m^{-2}\,s^{-1}$]
I local radiant intensity [$J\,m^{-2}\,s^{-1}$]
I^* equation (13)
K local thermal conductivity, equation (5) [$J\,m^{-1}\,s^{-1}\,K^{-1}$]
k radiation absorption coefficient [$m^2\,kg^{-1}$]
$\mathscr{R}$ ideal gas constant [$J\,kg^{-1}\,K^{-1}$]
R chemical rate coefficient, equation (8) [s^{-1}]
T local temperature [K]
T^* equation (13)
t time [s]
t^* equation (12)
V recession speed [$m\,s^{-1}$]
V^* equation (23)
V_0^* equation (38)
X laboratory-fixed coordinate [m]
X^* equation (12)
x moving coordinate [m]
x^* equation (23)
Y mass fraction, equation (13).

Greek symbols

γ equation (30)
μ equation (3)
ν equation (15)
ξ equation (29)
ρ local density [$kg\,m^{-3}$]
σ Stefan–Boltzmann constant [$J\,m^{-2}\,s^{-1}\,K^{-4}$].

INTRODUCTION

THERE are many practical applications in which a solid is heated by intense radiation. Laser–solid interactions provide one area [1]. Others are fire prevention, ramjet engines, atomic blasts and high-speed entry into Jupiter's atmosphere. Typically, gas evolves endothermically from the solid. This is the familiar basis of ablative cooling in thermal protection systems. In-depth absorption of radiation is also typical, not only for semi-transparent materials [2] but for apparently opaque ones as well [3–5].

We have taken a new approach to the problem of endothermic gasification of a solid by radiation absorbed in depth. Our model better describes the in-depth gas formation and avoids the common assumption that the reaction takes place at a prescribed temperature in an infinitely thin surface. We describe in a more sophisticated way how heat conduction and radiation absorption are coupled to the progress of the reaction. This approach actually simplifies the computation by avoiding a moving boundary whose location would be an extra unknown [6]. The model predicts a surface temperature given by a simple explicit formula. The surface temperature depends on the absorption coefficient, a fact that has been obscured in previous treatments. During steady recession, the temperature rises monotonically through the reaction zone whereas simpler models have predicted an interior temperature maximum.

The important features of the model are the

† Author to whom correspondence should be addressed.

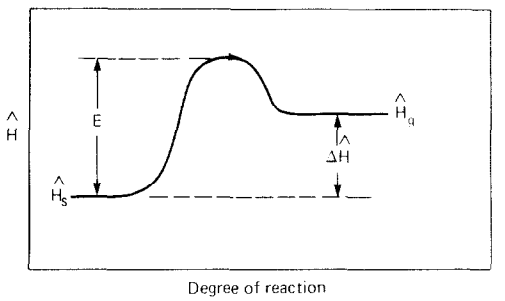

FIG. 1. The activation barrier.

following. The solid absorbs radiation in depth, inducing a solid-to-gas reaction that also occurs in depth. The gas escapes as rapidly as it is formed. The absorption coefficient and the thermal conductivity are both proportional to the local density. The reaction is controlled by an Arrhenius temperature-dependent rate coefficient [equation (8)]. The escaping gas carries sensible heat but there is no convective heat exchange with the solid.

Let us consider these points in detail. While heterogeneous reactions like $2C+O_2 \rightarrow 2CO$ may be confined near the surface, since they require a reactant available only in the gas phase, gas formation by phase change or chemical degradation can occur in depth, and may create cracks through which gas escapes, if channels are not already there. Many polymeric solids degrade into a porous matrix through which the gas can flow. This is especially true for composite materials consisting of a fiber matrix and a polymeric binder. In crystalline graphite gas escapes between basal planes in the lattice. If the solid forms a liquid layer, then the gas evolves as bubbles.

The assumption of rapid gas escape places an upper limit on the incident intensity. However, the limit is high based on the internal pressure [equation (40)]. Above the limit, spalling occurs.

With gas evolution in depth, the density of the solid varies smoothly through the reaction zone. Hence, it is necessary to include the density dependence of the absorption coefficient so the radiation intensity distribution will follow the density wave. The conductivity is set proportional to the density because it seems desirable that the conductivity should decrease to zero as the density decreases to zero. With conductivity proportional to density, the density drops out of the steady-state temperature equation.

The Arrhenius rate law allows gas to evolve realistically over a range of temperatures [7–10] and over a distributed zone. The use of an in-depth Arrhenius reaction avoids certain pitfalls. If the reaction is confined to a surface while the radiation penetrates the surface [11, 22], then the steady temperature distribution has an interior maximum. In practice, reaction rates increase as temperature increases, so that the reaction rate would then also have an interior maximum, which would be inconsistent with the neglect of in-depth gasification in such a model. Our model predicts that the steady temperature rises monotonically through the reaction zone, reaching an upper limit given by a simple explicit formula [equation (31)] that provides a natural definition of surface temperature. If the reaction and absorption are both confined to a surface [13] then the absorption coefficient plays no role [see equation (42)].

The Arrhenius law also allows the flexibility of an activation energy that is larger than the heat of reaction (Fig. 1). The difference is small for elemental materials like metals, but it can be important for polymer degradation [9, 10], and for overall reactions in which one activation energy is curve-fitted to a multistep process.

Our results are consistent with the neglect of heat exchange between gas and solid in that the gas evolves where the solid temperature is nearly uniform, so except for cooling on expansion, the two phases have nearly the same temperature where they make contact.

Our main emphasis is on the steady state, but we motivate our approach by starting with the full time-dependent problem. The detailed and overall governing equations are established and interpreted physically. The surface temperature formula and a good approximation to the recession speed are then obtained. After discussing the assumptions of the model for a wide range of real materials, including metals, graphite and plastics, we focus on plastics and calculate the initial response to an applied heat flux. The steady profiles of the temperature, density, in-depth intensity, reaction rate and absorption rate are then explored in detail to show the trends as the parameters of the problem are varied. This is followed by an examination of the surface temperature and recession speed, which is compared to previous calculations. Details of the mathematical techniques are available in ref. [14].

GOVERNING EQUATIONS

Consider a semi-infinite slab of material occupying the space $X \leqslant 0$ (Fig. 2), with radiation incident from the right. The heat balance equation may be written in

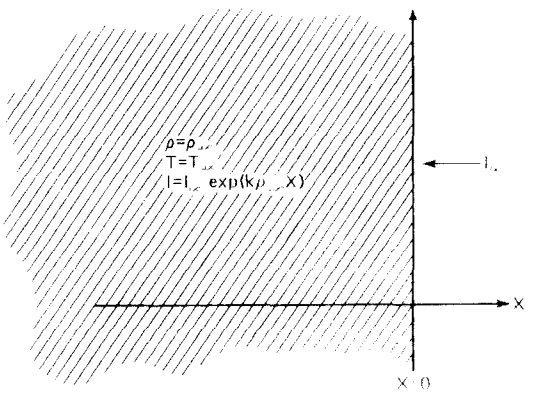

FIG. 2. Conditions at $t = 0$.

preliminary form as

$$\frac{\partial H}{\partial t} = \frac{\partial I}{\partial X} + \frac{\partial}{\partial X}\left(K\frac{\partial T}{\partial X}\right) + \hat{H}_g\frac{\partial \rho}{\partial t}, \quad X \leqslant 0. \tag{1}$$

The LHS is the rate of accumulation per unit volume of enthalpy in both solid and gas phases. The terms on the RHS are the contributions from absorption of radiation, heat conduction, and gas escape. Our assumptions discussed above are incorporated here: the gas that evolves in depth escapes as rapidly as it is formed and immediately dissipates its pressure, making a negligible contribution to the absorption and conduction terms. With the concentration of gas kept low, most of the enthalpy H per unit volume is due to the solid phase. We can write

$$\frac{\partial H}{\partial t} \approx \frac{\partial}{\partial t}(\rho \hat{H}_s) = \rho \hat{C}_s\frac{\partial T}{\partial t} + \hat{H}_s\frac{\partial \rho}{\partial t}, \tag{2}$$

and combine terms in $\partial\rho/\partial t$ to introduce the heat of reaction

$$\Delta\hat{H} \equiv \hat{H}_g - \hat{H}_s. \tag{3}$$

The heat balance equation is now

$$\rho\hat{C}_s\frac{\partial T}{\partial t} = \frac{\partial I}{\partial X} + \frac{\partial}{\partial X}\left(K\frac{\partial T}{\partial X}\right) + \Delta\hat{H}\frac{\partial \rho}{\partial t}. \tag{4}$$

For simplicity we assume that $\hat{C}_s$ and $\Delta\hat{H}$ are constants. We put

$$K = K_{-\infty}\rho/\rho_{-\infty} \tag{5}$$

where $K_{-\infty}$ is a constant. The radiation absorption law is

$$\frac{\partial I}{\partial X} = k\rho I, \tag{6}$$

where k is the density-based absorption coefficient. The mass balance is

$$\frac{\partial \rho}{\partial t} = -R\rho, \tag{7}$$

where the rate coefficient R has the usual Arrhenius temperature dependence

$$R = A\exp(-E/\mathscr{R}T) \tag{8}$$

in terms of an activation energy E and a frequency factor A.

The initial conditions are

$$T = T_{-\infty}, \quad \rho = \rho_{-\infty} \quad \text{at} \quad t = 0. \tag{9}$$

The boundary conditions at subsequent times are

$$I = I_\infty, \quad K\frac{\partial T}{\partial X} = 0 \quad \text{at} \quad X = 0, \tag{10}$$

$$\rho \to \rho_{-\infty}, \quad T \to T_{-\infty} \quad \text{as} \quad X \to -\infty. \tag{11}$$

We now rewrite the governing equations in nondimensional form. The new variables carry an asterisk (*) and are discussed from a physical viewpoint at the end of this section. Let

$$X^* = k\rho_{-\infty}X, \quad t^* = \frac{I_\infty k}{\Delta\hat{H}}t, \tag{12}$$

$$T^* = \frac{\hat{C}_s}{\Delta\hat{H}}T, \quad I^* = \frac{I}{I_\infty}, \quad Y = \frac{\rho}{\rho_{-\infty}}, \tag{13}$$

$$R^* = \nu\,\mathrm{e}^{-E^*/T^*}, \tag{14}$$

$$E^* = \frac{\hat{C}_s E}{\mathscr{R}\Delta\hat{H}}, \quad \nu = \frac{A\Delta\hat{H}}{I_\infty k}, \quad \mu = \frac{I_\infty\hat{C}_s}{K_{-\infty}\Delta\hat{H}k\rho_{-\infty}}. \tag{15}$$

Then the differential equations become

$$\mu\frac{\partial T^*}{\partial t^*} = \mu(I^* - R^*) + \frac{1}{Y}\frac{\partial}{\partial X^*}\left(Y\frac{\partial T^*}{\partial X^*}\right), \tag{16}$$

$$\frac{\partial I^*}{\partial X^*} = YI^*, \tag{17}$$

$$\frac{\partial Y}{\partial t^*} = -R^*Y. \tag{18}$$

The initial conditions are

$$T^* = T^*_{-\infty}, \quad Y = 1 \quad \text{at} \quad t^* = 0, \tag{19}$$

and the boundary conditions are

$$I^* = 1, \quad Y\frac{\partial T^*}{\partial X^*} = 0 \quad \text{at} \quad X^* = 0, \tag{20}$$

$$Y \to 1, \quad T^* \to T^*_{-\infty} \quad \text{as} \quad X^* \to -\infty. \tag{21}$$

The governing equations for steady recession may be written in new coordinates

$$x = X + Vt, \tag{22}$$

moving to the left at the unknown recession speed V that is eventually attained: we define

$$V^* = \frac{\Delta\hat{H}\rho_{-\infty}V}{I_\infty}, \quad x^* = k\rho_{-\infty}x. \tag{23}$$

Then the equations become (after dropping time derivative terms)

$$\frac{\mathrm{d}^2T^*}{\mathrm{d}x^{*2}} - \left(\mu V^* + \frac{R^*}{V^*}\right)\frac{\mathrm{d}T^*}{\mathrm{d}x^*} + \mu(I^* - R^*) = 0, \tag{24}$$

$$\frac{\mathrm{d}I^*}{\mathrm{d}x^*} = YI^*, \tag{25}$$

$$\frac{\mathrm{d}Y}{\mathrm{d}x^*} = -\frac{R^*}{V^*}Y, \tag{26}$$

subject to the boundary conditions

$$I^* \to 1, \quad Y\frac{\mathrm{d}T^*}{\mathrm{d}x^*} \to 0 \quad \text{as} \quad x^* \to \infty, \tag{27}$$

$$Y \to 1, \quad T^* \to T^*_{-\infty} \quad \text{as} \quad x^* \to -\infty. \tag{28}$$

These conditions are sufficient up to translation to determine T^*, I^*, Y, and V^*. (A special relation for computing V^* from other quantities is derived below.)

Note that the steady recession problem is defined over the whole interval $-\infty < x^* < \infty$, and there is no

abrupt surface. However, we will see that most of the drop in density occurs in a very narrow interval, and the residual material is so sparse that its influence is completely negligible. In practice, the residual solid would collapse or blow away.

Notice, too, that the location of the origin is arbitrary. We are free to assign any reasonable value to Y or I^* or T^* at $x^* = 0$. However, we will do so indirectly. In solving the steady equations, we first guess approximate solutions and then make corrections. Our guesses, being explicit functions of x, have a built-in choice of origin. The computations suggest that successive approximations converge without shifting along the x-axis.

For steady recession to exist, we require that the reaction rate at the limit temperature $T_{-\infty}$, be negligibly small. This condition is automatically met at room temperature for practical rate parameters. Formally, we can replace the Arrhenius function $R(T)$ by zero below some cutoff temperature near $T_{-\infty}$ and make the transition smooth.

It is helpful to discuss briefly the physical interpretation of the nondimensional variables and parameters. The time variable t^* is based on the characteristic time $\Delta\hat{H}/kI_\infty$ required to absorb enough radiant heat in a volume to gasify the solid contained in this volume. The coordinate x^* is defined in terms of a rough radiation penetration depth $1/k\rho_{-\infty}$. We will also use a coordinate

$$\xi = \mu x^* = \frac{1}{V^*}\frac{x}{K_\infty/(\rho_{-\infty}\hat{C}_s V)}, \tag{29}$$

closely related (since $V^* \approx 1$) to the penetration depth $K_{-\infty}/\rho_{-\infty}\hat{C}_s V$ of the conductive thermal wave into the advancing solid. The intensity and density are both referred to asymptotic values which makes Y the mass fraction. The temperature unit $\Delta\hat{H}/\hat{C}_s$ is a temperature at which the sensible heat is sufficient for complete gasification. The parameter ν is the ratio of a rate $A\Delta\hat{H}$ at which energy is consumed by the reaction (at infinite temperature) to a rate kI_∞ at which radiant energy is absorbed. Note that the reaction rate actually attained is smaller than A by many orders of magnitude. An alternate interpretation of ν is the ratio of the new time unit $\Delta\hat{H}/kI_\infty$ to a reaction time A^{-1} (at infinite temperature). When $\nu \leqslant 1$, the reaction is overwhelmed by radiation and no steady states exist. The quantity μ may be thought of as a reciprocal conductivity in the new units. The parameter μV^* is the ratio of the absorption depth to the depth of the conductive thermal wave. (Since $V^* \approx 1$, μ may also be interpreted in this way.) When $\mu V^* > 1$, the asymptotic thermal wave is controlled by radiation and convection. When $\mu V^* < 1$, conduction and convection are controlling. The quantity

$$\gamma = \nu/\mu, \tag{30}$$

is obtained by dividing an approximate time $K_{-\infty}\rho_{-\infty}(\Delta\hat{H})^2/\hat{C}_s I_\infty^2$ to reach steady state (see discussion of Table 2) by a chemical reaction time $1/A$ at infinite temperature.

OVERALL BALANCES

The mathematical investigation [14] of the steady-state equations (24)–(28) reveals the interesting result that the steady temperature rises monotonically with x^* from $T^*_{-\infty}$ to a finite upper limit of remarkable and elegant simplicity

$$T^*_\infty = E^*/\ln \nu, \tag{31}$$

corresponding to $R^* = 1$, provided $\nu > 1$. While there is no abrupt surface in our model, it is natural to define T^*_∞ as a 'surface temperature'. Note that equation (31) expresses T^*_∞ in terms of the incident intensity and the absorption coefficient through ν.

The formula for V^* is obtained from the steady overall balance equations for heat, radiation intensity and mass. We begin by rearranging the temperature equation (24) as

$$\frac{1}{\mu}\frac{\mathrm{d}}{\mathrm{d}x^*}\left(Y\frac{\mathrm{d}T^*}{\mathrm{d}x^*}\right) - V^*\frac{\mathrm{d}}{\mathrm{d}x^*}(YT^*) + V^*T^*\frac{\mathrm{d}Y}{\mathrm{d}x^*} + I^*Y - R^*Y = 0. \tag{32}$$

Each term is a rate of accumulation of heat per unit volume in the units $k\rho_{-\infty}I_\infty$. In order of appearance the terms describe conduction, convection of sensible heat by the solid, sensible heat removed by the gas, radiation, and reaction. On integration, the conduction has no net effect and we obtain

$$V^*T^*_{-\infty} + \int_{-\infty}^{\infty} I^*Y\,\mathrm{d}x^* = \int_{-\infty}^{\infty} R^*Y\,\mathrm{d}x^* - \int_{-\infty}^{\infty} V^*T^*\frac{\mathrm{d}Y}{\mathrm{d}x^*}\mathrm{d}x^*. \tag{33}$$

Thus, the total heat imparted by convection of sensible heat in the incoming solid and absorption of radiation (terms on the LHS) is partly consumed by the reaction and partly removed by the gas (terms on the RHS). We note that the gas term is

$$-\int_{-\infty}^{\infty} V^*T^*\frac{\mathrm{d}Y}{\mathrm{d}x^*}\mathrm{d}x^* = V^*T^*_\infty - V^*\int_{-\infty}^{\infty}(1-Y)\frac{\mathrm{d}T^*}{\mathrm{d}x^*}\mathrm{d}x^*. \tag{34}$$

The total rate at which radiant heat is absorbed is

$$\int_{-\infty}^{\infty} I^*Y\,\mathrm{d}x^* = 1, \tag{35}$$

from equation (25). This is the overall balance for radiant intensity. The total rate at which the reaction absorbs heat is

$$\int_{-\infty}^{\infty} R^*Y\,\mathrm{d}x^* = V^*, \tag{36}$$

from equation (26). This is the overall mass balance.

Substituting into equation (33) gives the formula

$$V^* = \left[1 + T^*_\infty - T^*_{-\infty} - \int_{-\infty}^{\infty} (1-Y)\frac{dT^*}{dx^*}\,dx^*\right]^{-1}. \tag{37}$$

This formula is used in the numerical calculations. We will see, however, that the integral here is very small because most of the temperature rise occurs where $Y \approx 1$. Hence the quantity

$$V^*_0 \equiv \frac{1}{1 + T^*_\infty - T^*_{-\infty}}, \tag{38}$$

is a reasonable approximation to the recession speed V^*. Formula (38) is equivalent to the approximation [13]

$$I_\infty \approx \rho_{-\infty} V[\Delta\hat{H} + \hat{C}_s(T_\infty - T_{-\infty})].$$

NUMERICAL METHODS

We approximate the solution to the time-dependent problem of equations (16)–(21) by finite differences. We use a modification of the Crank–Nicholson method [15, pp. 141–143], solving for T^* and R^* at integral time steps $j\tau$, where τ is a small step-width, and finding Y and I^* at half-integral time-steps, $(j+\frac{1}{2})\tau$. Given Y and I^* at a particular half-step, we solve for T^* at the next integral step by approximating $\partial T^*/\partial t^*$ in equation (16) by a time difference and $(1/Y)(\partial/\partial X^*)(Y\,\partial T^*/\partial X^*)$ by an average over the adjacent time-steps of centered space differences. R^* is also averaged over the time-steps. With appropriate use of the boundary conditions, this gives an implicit relation for the new values of T^* at the advanced time-step. R^* is linearized at the advanced time-step to give a linear tridiagonal system which is easily solved. Once T^* is found, R^* is immediately determined. Then Y and I^* are evaluated at the next half-step by simple difference approximations of equations (17) and (18).

The solution of the steady recession equations (24)–(28) may be obtained by an iterative scheme. The second condition in equation (27) is replaced by equation (31). For given approximations to V^* and I^*, equation (24) and its boundary conditions constitute a nonlinear two-point boundary value problem which may be solved for dT^*/dx and T^* by a suitable numerical method. From T^* and the corresponding R^*, we numerically integrate equation (26) to get Y and then integrate equation (25) to get a new approximation to I^*; integration constants follow from equations (27) and (28). Finally, using dT^*/dx^* and Y, we obtain a new V^* from equation (37). The entire sequence is repeated until differences between successive approximations become negligible. The starting approximations used are

$$V^* \approx V^*_0, \tag{39}$$

and

$$I^* \approx \begin{cases} \exp[-V^*_0 + x^*], & x^* \leqslant 0, \\ \exp[-V^*_0\, e^{-x^*/V^*_0}], & x^* \geqslant 0. \end{cases}$$

For numerical solution of equations (24), (27) and (28), we replace the boundary conditions at $x^* = \pm\infty$ by approximately equivalent conditions at certain finite values of x^* which can be obtained from the asymptotic behavior of the solution. A simple difference method is applied that leads to a nonlinear tridiagonal system of equations which can be solved iteratively by Newton's method [16] for the temperature values. This involves expanding $R^*(T^*)$ about the old approximation for T^* and keeping only linear terms to solve for the new approximation.

For more details on the numerical methods and on the asymptotic behavior of the solutions, see ref. [14].

APPLICABILITY OF THE MODEL

In this section, we introduce some real materials under practical radiation intensities. We show that the assumptions of the model are satisfied over a wide range of conditions and that steady recession is easily attained.

Table 1 lists nominal values of the required properties for four materials. The two plastics are polymeric materials, one semi-transparent and the other absorbing like graphite. The plastics also represent composite materials in an average sense.

Table 2 shows some typical cases in which the materials are exposed to radiation. The incident intensity I_∞ is given in the first column and the reradiated intensity σT^4_∞ is in the second column. The group $\Delta\hat{H}/kI_\infty$ is an approximate time required to absorb enough heat to gasify a unit mass of solid, and is taken as the time unit for the non-dimensional

Table 1. Material properties

	ATJ-graphite	Aluminum	Plastics
$\hat{C}_s$ [J kg^{-1} K^{-1}]	8.4×10^2	8.4×10^2	1.5×10^3
$E/\mathscr{R}$ [K]	8.56×10^4	4.0×10^4	1.9×10^4
$K_{-\infty}$ [W m^{-1} K^{-1}]	1×10^2	2.4×10^2	4×10^{-1}
A [s^{-1}]	3.2×10^{13}	8.1×10^{12}	5×10^{13}
k [m^2 kg^{-1}]	1.5×10^3	3.1×10^4	7×10^{-1}
			1.5×10^3
$T_{-\infty}$ [K]	3×10^2	3×10^2	3×10^2
$\Delta\hat{H}$ [J kg^{-1}]	5.93×10^7	1.22×10^7	4×10^6
$\rho_{-\infty}$ [kg m^{-3}]	1.73×10^3	2.70×10^3	2×10^3

Table 2. Typical cases

	I_∞	σT_∞^4	$\frac{\Delta\hat{H}}{kI_\infty}$	$\frac{I_\infty}{\rho_{-\infty}\Delta\hat{H}}$	$\frac{K_{-\infty}\rho_{-\infty}(\Delta\hat{H})}{\hat{C}_s I_\infty^2}$
	[W m^{-2}]	[W m^{-2}]	[s]	[m s^{-1}]	[s]
Graphite	1.0×10^{8}	1.0×10^{7}	4.0×10^{-4}	9.7×10^{-4}	6.7×10^{1}
	5.0×10^{12}	1.3×10^{8}	8.0×10^{-9}	4.9×10^{1}	2.7×10^{-8}
Aluminum	3.3×10^{7}	1.3×10^{6}	1.2×10^{-5}	1.0×10^{-3}	1.1×10^{2}
	5.0×10^{12}	8.9×10^{7}	7.9×10^{-11}	1.5×10^{2}	4.8×10^{-9}
Plastics	2.0×10^{5}	5.3×10^{3}	2.9×10^{1}	2.5×10^{-5}	2.1×10^{2}
($k = 7.0\times10^{-1}$ m^2 kg^{-1})	5.0×10^{6}	7.7×10^{3}	1.2	6.3×10^{-4}	3.4×10^{-1}
	2.0×10^{10}	2.5×10^{4}	2.9×10^{-4}	2.5	2.1×10^{-8}
Plastics	2.0×10^{5}	1.4×10^{4}	1.3×10^{-2}	2.5×10^{-5}	2.1×10^{2}
($k = 1.5\times10^{3}$ m^2 kg^{-1})	5.0×10^{6}	2.3×10^{4}	5.3×10^{-4}	6.3×10^{-4}	3.4×10^{-1}
	6.7×10^{10}	1.7×10^{5}	4.0×10^{-8}	8.4	1.9×10^{-9}

variables. The fourth column is an approximate recession speed corresponding to $V^* = 1$. The last column is an approximate adaptation time to reach steady state derived from a simple model [17] in which the solid is moving in the positive x-direction at speed $\Delta\hat{H}/kI_\infty$. The plane $x = 0$ is maintained at temperature T_∞. At time zero, the solid temperature is $T_{-\infty}$. The true adaptation time was calculated in one case (plastics, $k = 0.7$ m^2 kg^{-1}, $I_\infty = 2.0\times10^5$ W m^{-2}) and found to agree closely with the estimated value.

The highest intensity values listed are attainable with common pulsed lasers and the intermediate values are obtained with continuous lasers. The value of 5.0×10^6 W m^{-2}, is possible in intense house fires. In all cases the intensity can be maintained for the time required to reach steady state, column 5, and is below the plasma threshold.

It is interesting to note that adaptation times at high intensities are remarkably small. The gasification times in column 3 are sometimes even smaller.

The neglect of reradiation is justified by column 2. Here the reradiated intensities are below the incident intensities by at least a factor of 10.

It is not clear whether corrections may be necessary for gas absorption. The incident intensities are below the plasma threshold. However, some of the recession speeds in column 4 are very high, implying high gas evolution rates.

High evolution rates also raise the question of subsurface pressure build-up. The gas pressure is required to be low in equations (1) and (2) but in addition, the pressure should not exceed the strength of the solid. What internal pressure is required to drive out the gas as rapidly as we have assumed? To make a representative calculation, we apply Darcy's law [18] in the form

$$\Delta P = -\frac{\mu_g v_g}{k_s}\Delta x = -\frac{\mu_g(\rho_g V_g)\Delta x}{k_s\rho_g}, \qquad (40)$$

with the gas viscosity $\mu_g = 1\times10^{-5}$ kg m^{-1} s^{-1}, the permeability k_s taken to be 1×10^{-10} m^2 [18], the mass flux of gas $\rho_g v_g$ set equal to the solid flux ρV estimated from the approximate recession speed in Table 2, namely, $\rho V = I_\infty/\Delta\hat{H}$, the gas density ρ_g set conservatively at $\rho_g = 0.7$ kg m^{-3}, and Δx taken to be the radiation penetration depth $\Delta x = 1/k\rho_{-\infty}$. Then the highest excess pressure that arises in Table 2 (plastics, $k = 7.0\times10^{-1}$ m^2 kg^{-1}, $I_\infty = 2.0\times10^{10}$ W m^{-2}) is $\Delta P = 5$ atm. This is low enough for equations (1) and (2) but undoubtedly approaches the pressure the solid can withstand. In the other cases in Table 2, the internal pressure is much less. In general, the last calculation may be applied to estimate the onset of spalling as intensity is varied.

TRANSIENT DISTRIBUTIONS

Figure 3 shows the initial response of a semi-transparent plastic with $k = 0.7$ m^2 kg^{-1} and $I_\infty = 2.0\times10^5$ W m^{-2} (see Table 2). Distributions of Y^*, I^* and T^* are shown at equal time intervals in stationary coordinates.

At time zero the surface is abrupt, Y is a step-function, and I is an exponential decay given by $I = I_\infty \exp(-k\rho_{-\infty}X)$. After about 30 s ($t^* = 1$), Y has dropped by about 50% at the original surface, gas is evolving to a depth of about 1 mm, and the surface becomes diffuse. After 250 s ($t^* = 8$), Y has made a smooth transition from $Y = 1$ to essentially zero at $X = 0$ and steady recession is established. The reaction is then distributed over a thickness of about 2 mm.

As soon as ablation begins the intensity distribution departs significantly from an exponential decay. Since the density dependence of absorption is included in our model, the intensity can adapt to the changing density distribution and follow it as steady recession develops. The temperature also adapts to the onset of ablation through the strong coupling to Y and I^*. The coupling arises through the reaction heat consumption, through radiation absorption, and finally through heat conduction, since our model includes the concentration dependence of the conductivity.

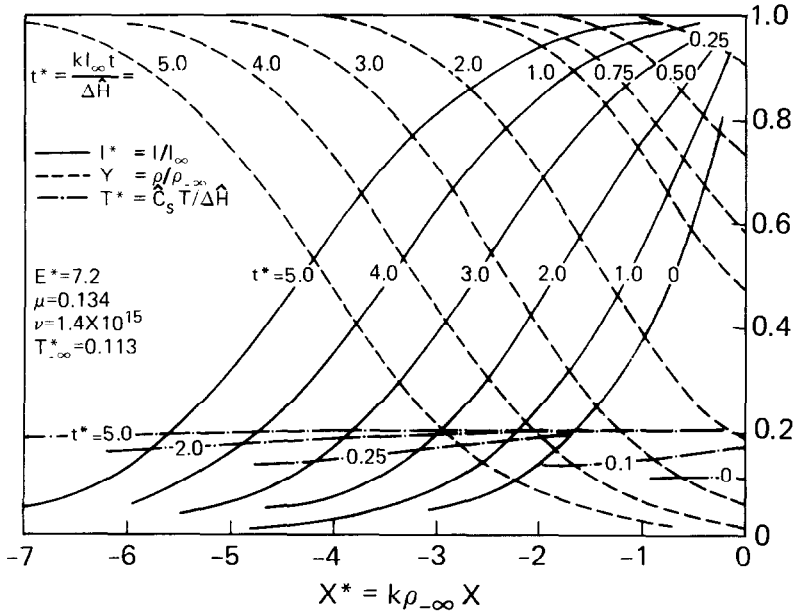

FIG. 3. Approach to steady recession.

TRENDS IN STEADY RECESSION

In this section, we still consider plastic materials (Table 1) but show steady distributions in moving coordinates. It should be noted that the origin is fixed only by the computational procedure and not by any physical condition, so comparison of curves is possible up to translation only.

In Fig. 4, the incident intensity is $I_\infty = 5\times10^6$ W m^{-2} and the absorption coefficient is varied. The steady temperature wave does not show the internal maximum predicted by simpler models in which the traveling reaction zone is infinitely thin [11–13]. Instead, T^* rises monotonically and approaches T^*_∞ (the dashed lines) as $Y \to 0$.

Although the surface is diffuse in our model, we have defined the temperature limit T^*_∞ to be the surface temperature. This is justified by comparing the T^* and Y charts in Fig. 4. One sees that the temperature essentially attains its upper limit while there is still a significant amount of solid left.

The rise in temperature shown in Fig. 4 is due ultimately to the absorption of radiation. The rise is greater when k increases and more radiation is absorbed. For comparison, Fig. 4 shows the rate I^*Y at which radiation is absorbed per unit volume in units of $k\rho_{-\infty}I_\infty$. The area under each curve is μ, from equations (29) and (35). For each k the location of the zone where radiation is absorbed roughly matches the location of greatest temperature rise. To the interior of the absorption zone T^* is independent of k. Note that the absorption zone is narrow for large k and broader for small k.

Figure 4 also shows the rate R^*Y at which the reaction consumes heat per unit volume, in units of $k\rho_{-\infty}I_\infty$. The area under each curve is μV^*, from equations (29) and (36). Since μV^* is usually close to μ, which is the area under the absorption curves, most of the heat absorbed is consumed by the reaction. The location of the reaction zone also corresponds to that of the absorption zone. We do observe, however, that conduction reduces the peak value of the R^*Y curve when μ is small, i.e. conduction moves the absorbed heat before it is consumed by reaction.

Finally, in Fig. 4, R^*Y may also be interpreted as the mass rate of evolution of gas per unit volume, in units of $I_\infty k\rho_{-\infty}/\Delta\hat{H}$. A comparison of the Y and R^*Y curves shows that the gas evolution rate is highest where Y is 20–50%. Our model assumes that the gas can escape through the remaining space before the pressure builds up. When the evolution rate is too high, cf. equation (40), spalling occurs, and flakes of the solid are blown off.

Figure 5 shows the intensity distribution for various absorption coefficients k and incident intensities I_∞. For an abrupt surface in which Y is a step-function, I^* would be simply $\exp(x^*)$ and all the curves would coincide. Then the in-depth intensity I would be proportional to I_∞ and the penetration depth proportional to $1/k$. With a diffuse surface the proportionalities are lost. We note that when μ is large enough, say $\mu > 10$, then $I^* \to R^*$ for positive x^*.

SURFACE TEMPERATURE, RECESSION SPEED AND GAS FLUX

The steady 'surface temperature' T_∞ is plotted in Fig. 6. Note from equations (13), (15) and (31) that T_∞ is independent of the density $\rho_{-\infty}$ and the thermal properties $K_{-\infty}$ and $\hat{C}_s$, but it depends on all the other parameters of the problem. In particular, T_∞ depends on the product kI_∞, which is a rate of absorption of

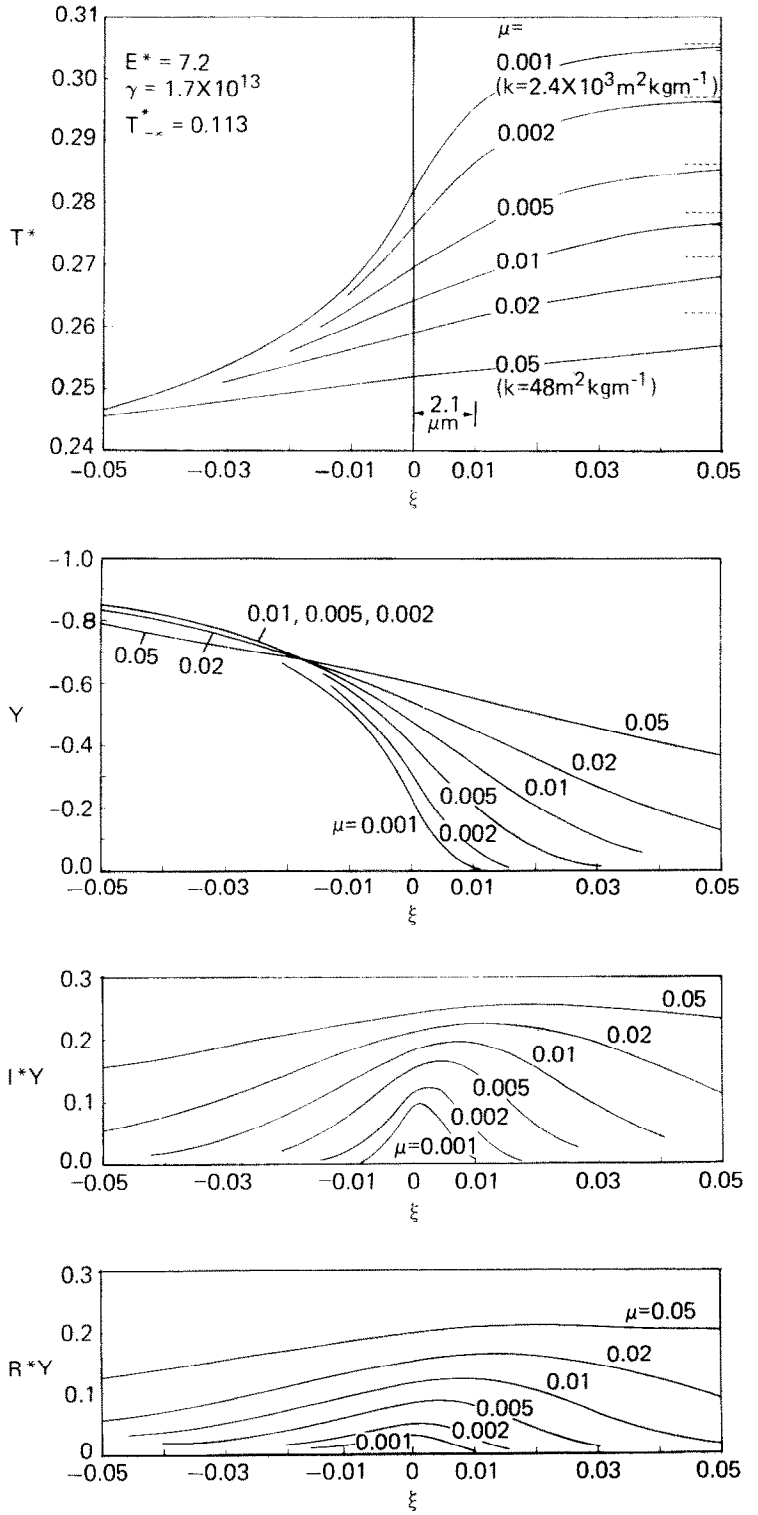

FIG. 4. Comparison of some steady profiles.

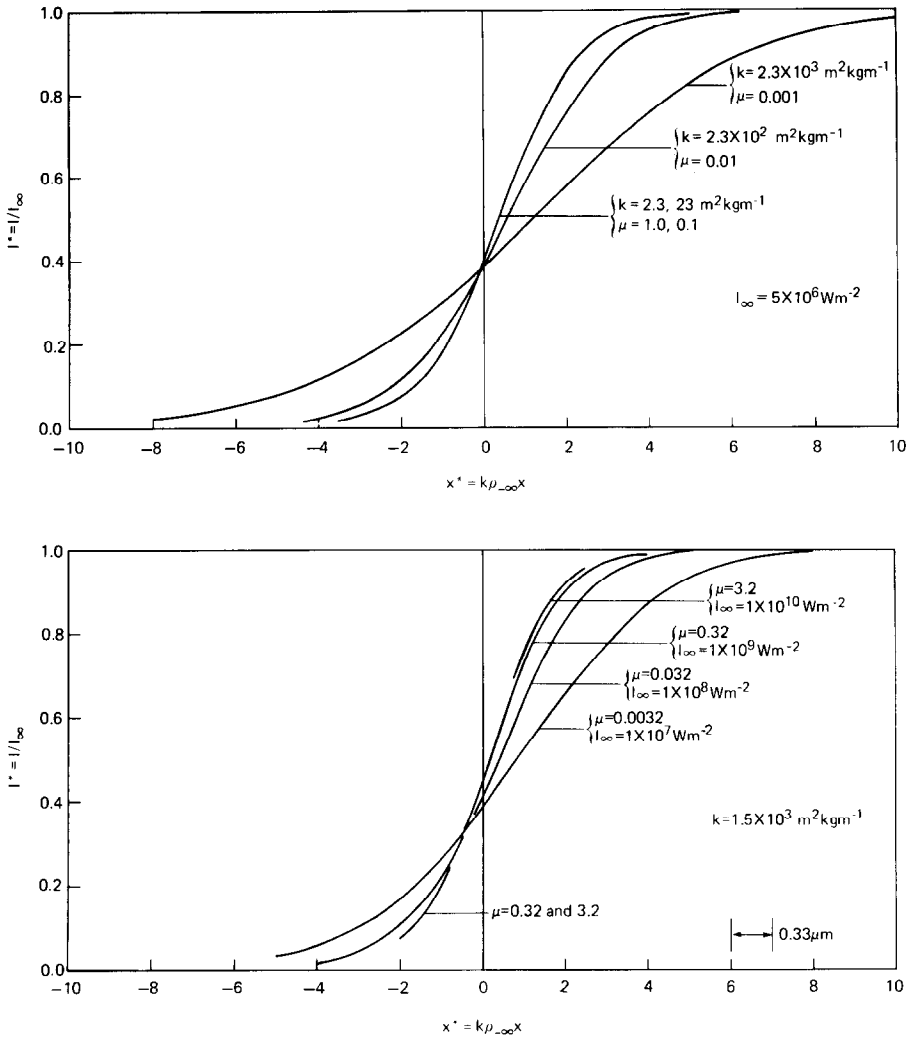

FIG. 5. Steady in-depth intensity.

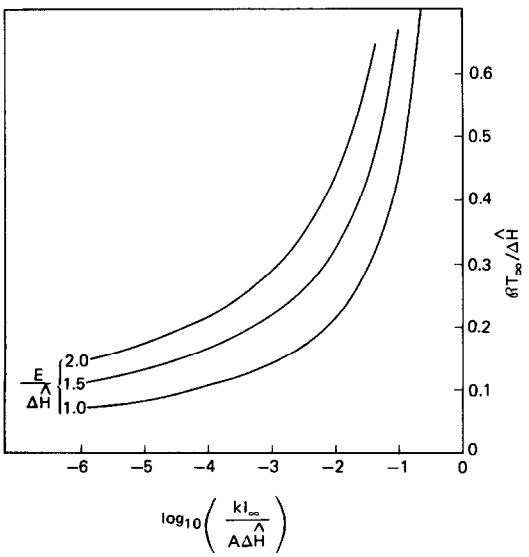

FIG. 6. Steady surface temperature.

radiation per unit mass. As kI_∞ rises, so does T_∞. At very large kI_∞, corresponding to $v = 1$, steady recession no longer exists and $T_\infty \to \infty$. [Before this condition is reached, our model would lose its applicability because the gas evolution rate (see below) would become too large.] In addition to kI_∞, the activation energy E has a very large effect on the surface temperature.

The recession speed V is given to good accuracy by V_0, the deviation being less than 4% in one series of calculations. The total mass flux of gas is just $\rho_{-\infty}V$. Figure 7 shows the rise in V_0 as I_∞ increases. Again, when I_∞ is too large, either steady states no longer exist or $\rho_{-\infty}V$ becomes too large for the model. The curves are labelled by the value of $\hat{C}_s/\mathscr{R}$. For many metals, $\hat{C}_s/\mathscr{R} \simeq 3$. Figure 8 shows the dependence of V_0 on the kinetic parameters A and E and the absorption coefficient k. The model can break down in the vicinity of the origin in this figure. Most practical cases are away from this region making V_0 roughly independent of A and k but still strongly dependent on E.

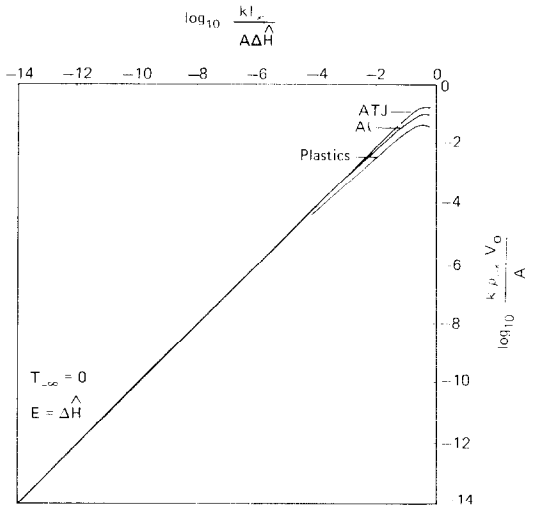

FIG. 7. Steady recession speed.

Formulas (31) and (38) for T_∞ and V_0, may be combined to give V_0 in terms of the surface temperature

$$V_0 = \frac{A}{k\rho_{-\infty}} \frac{\exp(-E/\mathscr{R}T_\infty)}{[1+\hat{C}_s(T_\infty - T_{-\infty})/\Delta\hat{H}]}. \tag{41}$$

Here we have eliminated the intensity I_∞ of the incident beam but its wavelength distribution still has an influence through the absorption coefficient k.

The last formula may be directly compared with earlier results. Ready's analysis [13] of the vaporization of metals is based on equation (39) and

$$V = h_a A \exp(-\Delta\hat{H}/\mathscr{R}T_\infty), \tag{42}$$

where h_a is the thickness of an atomic layer in the crystal lattice. The last result may be derived by statistical mechanics [19] on the assumption that only the atoms in the outermost layer can escape. If we approximate the square bracket in equation (41) by 1 and set $E = \Delta\hat{H}$, then the temperature dependence is the same as in equation (42). It follows that Ready's results are a special case of ours in which $E = \Delta\hat{H}$ and the penetration depth is the thickness of one layer

$$\frac{1}{k\rho_{-\infty}} = h_a. \tag{43}$$

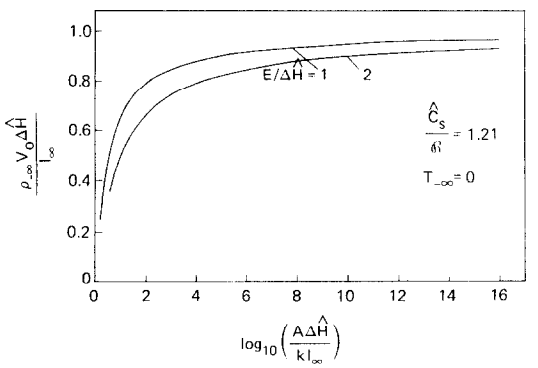

FIG. 8. Steady recession speed.

Kindelan and Williams [12, 20] write

$$V = Be^{-E/\mathscr{R}T_\infty}, \tag{44}$$

and leave B as a free parameter. Their reaction occurs at an abrupt surface and B is assumed to be independent of the absorption coefficient k. Based on these assumptions, the authors conclude that their surface temperature, which depends on B, is independent of k. Replacing their reaction with a distributed one, we would interpret B from equation (41) with the square bracket again set equal to 1

$$B = \frac{A}{k\rho_{-\infty}}. \tag{45}$$

With this interpretation, B, as well as the surface temperature, would depend on k, just as we have found. The authors thank one of the referees for pointing out a paper [21] that considers simultaneous in-depth absorption and in-depth Arrhenius reaction. However, the reaction is exothermic rather than endothermic and hence the problem is fundamentally different.

The Langmuir equation [7] for the mass flux of gas, which determines the recession speed, is inappropriate in this problem. The equation is derived by equating the mass flux to that leaving the solid when in equilibrium with a vapor, which in turn is the condensation flux. However, a solid exposed to radiant heating is experiencing conditions that can be quite different from those experienced in equilibrium. It must be assumed first that the temperature gradient in the solid is small, since at equilibrium the gradient is zero. In addition, polymeric materials are normally incapable of reaching equilibrium with a vapor since they decompose irreversibly.

CONCLUSION

We find the surprising result that the steady surface temperature of an ablating solid has a much simpler form when the calculation includes processes that have been neglected before. The surface temperature is given explicitly by

$$T_\infty = E/\mathscr{R} \ln\left(\frac{A\Delta\hat{H}}{I_\infty k}\right). \tag{46}$$

The model includes in-depth absorption of radiation at a rate proportional to the local density [see equation (6)]. The effects are reflected in the formula through the incident intensity I_∞ and the density-based absorption coefficient k. The effect of the temperature dependence of the chemical rate coefficient is included through the activation energy E and the frequency factor A [see equations (7) and (8)]. The gas evolves in depth with a heat of reaction $\Delta\hat{H}$. The model also includes the density dependence of the conductivity, equation (5), and this contributes to the overall simplicity of the formula.

The presence of the absorption coefficient k in the formula is probably the most significant new feature.

With the common assumption that the reaction zone is infinitely thin, k does not appear at all.

Acknowledgements—The authors thank Mr Nathan Rubinstein for assistance in computing the charts. This work was supported by the Naval Sea Systems Command, U.S. Department of the Navy, under Contract N00024-81-C-5301.

REFERENCES

1. N. Bloembergen, Fundamentals of laser–solid interactions, *Laser–Solid Interactions and Laser Processing—1978* (edited by S. D. Ferris, H. J. Leamy and J. M. Poate), pp. 1–9. American Institute of Physics (1979).
2. R. Viskanta and E. E. Anderson, Heat transfer in semitransparent solids, *Adv. Heat Transfer* **11**, 317–441 (1975).
3. T. J. Ohlemiller and M. Summerfield, A critical analysis of arc image ignition of solid propellants, *AIAA J.* **6**, 878 (1968).
4. T. J. Ohlemiller and M. Summerfield, Radiative ignition of polymeric materials in oxygen/nitrogen mixtures, 13th Symp. (Int.) on Combustion, pp. 1087–1094. The Combustion Institute (1971).
5. T. Kashiwagi, A radiative ignition model of solid fuel, *Combust. Sci. Technol.* **8**, 225–236 (1974).
6. D. G. Wilson, A. D. Solomon and P. T. Boggs (editors) *Moving Boundary Problems*. Academic Press, New York (1978).
7. S. Dushman and J. M. Lafferty, *Scientific Foundations of Vacuum Technique*. Wiley, New York (1962).
8. S. L. Madorsky, *Thermal Degradation of Organic Polymers*. Krieger, New York (1975).
9. L. A. Wall, Pyrolysis of polymers, *The Mechanisms of Pyrolysis, Oxidation, and Burning of Organic Materials*, pp. 47–60. National Bureau of Standards Special Publication 357, Gaithersburg (1972).
10. L. A. Wall, Condensed phase combustion chemistry, *Fire Res. Abstr. Rev.* **13**, 204–219 (1971).
11. J. G. Boehringer and R. J. Spindler, Radiant heating of semitransparent materials, *AIAA J.* **1**, 84–88 (1963).
12. M. Kindelan and F. A. Williams, Gas-phase ignition of a solid with in-depth absorption of radiation, *Combust. Sci. Technol.* **16**, 47–58 (1977).
13. J. F. Ready, *Effects of High Power Laser Radiation*, pp. 106–109. Academic Press, New York (1971).
14. W. Börsch-Supan, L. W. Hunter and J. R. Kuttler, Endothermic gasification of a solid by thermal radiation absorbed in depth, M.S. Eisenhower Research Center Report, Applied Physics Laboratory (1982).
15. G. F. Forsythe and W. R. Wasow, *Finite Difference Methods for Partial Differential Equations*. Wiley, New York (1960).
16. S. G. Mikhlin and K. L. Smolitskiy, *Approximate Methods for Solution of Differential and Integral Equations*, p. 12. Elsevier, Amsterdam (1967).
17. H. S. Carslaw and J. C. Jaeger, *Conduction of Heat in Solids* (2nd edn.), p. 388. Clarendon Press, Oxford (1959).
18. R. R. Rumer, Jr., Resistance of flow through porous media, in *Flow through Porous Media* (edited by R. J. M. DeWiest), pp. 91–108. Academic Press, New York (1969).
19. J. Frenkel, *Kinetic Theory of Liquids*, p. 5. Clarendon Press, Oxford (1946).
20. M. Kindelan and F. A. Williams, Theory for endothermic gasification of a solid by a constant energy flux, *Combust. Sci. Technol.* **10**, 1–19 (1975).
21. M. M. Ibiricu and F. A. Williams, Influence of externally applied thermal radiation on the burning rates of homogeneous solid propellants, *Combust. Flame* **24**, 185–198 (1975).

GAZEIFICATION ENDOTHERMIQUE D'UN SOLIDE PAR UN RAYONNEMENT THERMIQUE ABSORBE EN PROFONDEUR

Résumé—Un solide est exposé à un rayonnement thermique qui pénètre la surface. Le solide est gazéifié en profondeur par une réaction endothermique avec un coefficient d'Arrhenius. L'absorption du rayonnement et la conduction thermique dépendent toutes les deux de densité locale. Les matériaux considérés sont des polymères solides, des composites, du graphite et des métaux. Le modèle estime une élévation de température monotone à travers la zone de réaction et une température de surface qui dépend du coefficient d'absorption. Ceci contredit des résultats antérieurs de chauffage par rayonnement, spécialement par laser à grande puissance.

ENDOTHERME VERGASUNG EINES FESTKÖRPERS DURCH IM INNERN ABSORBIERTE WÄRMESTRAHLUNG

Zusammenfassung—Ein Modell-Festkörper wird thermischer Strahlung ausgesetzt, die die Oberfläche durchdringt. Der Festkörper vergast im Innern durch eine endotherme Reaktion, die einer Arrhenius-Beziehung folgt. Sowohl die Strahlungs-Absorption wie auch die Wärmeleitfähigkeit sind von der örtlichen Dichte abhängig. Die betrachteten Materialien sind: polymere Festkörper, Verbundstoffe, Graphit und Metalle. Das Modell liefert einen monotonen Temperatur-Anstieg durch die Reaktionszone und eine Oberflächen-Temperatur, die vom Absorptions-Koeffizienten abhängt. Dies steht im Gegensatz zu früheren Berechnungsergebnissen für Strahlungs-Beheizung, insbesondere durch Hochenergie-Laser.

ЭНДОТЕРМИЧЕСКИЙ ПЕРЕХОД ТВЕРДОГО ТЕЛА В ГАЗООБРАЗНОЕ СОСТОЯНИЕ ЗА СЧЕТ ПОГЛОЩАЕМОГО ПО ГЛУБИНЕ ТЕПЛОВОГО ИЗЛУЧЕНИЯ

Аннотация—Исследовано воздействие на модельное твердое тело теплового излучения, проникающего через поверхность тела. В глубине тела происходит превращение твердого вещества в газ за счет эндотермической реакции, подчиняющейся закону Аррениуса. Как поглощение излучения, так и теплопроводность зависят от локальной плотности вещества. Исследовались полимерные твердые тела, композиты, графит и металлы. Согласно модели, температура в зоне реакции растет монотонно, а температура поверхности зависит от коэффициента абсорбции. Это противоречит результатам ранее проведенных расчетов лучистого нагрева особенно с помощью мощных лазеров.